Supporting information for

Nanoscale Electronic Inhomogeneity in In_2Se_3 Nanoribbons Revealed by Microwave Impedance Microscopy

Keji Lai[1], Hailin Peng[2*], Worasom Kundhikanjana[1], David T. Schoen[2], Chong Xie[2], Stefan Meister[2], Yi Cui[2], Michael A. Kelly[2], Zhi-Xun Shen[1]*

[1]*Department of Applied Physics, Stanford University, Stanford, CA 94305*

[2]*Department of Materials Science and Engineering, Stanford University, Stanford, CA 94305*

* *These authors contributed equally to this work.*

Correspondence and requests for materials should be addressed to Z.X.S. (zxshen@stanford.edu) or Y.C. (yicui@stanford.edu).

Method summary

The near-field scanning microwave impedance microscope is implemented on a commercial AFM platform (PacificNanotech Inc., PTrak2). The microwave is generated by a frequency synthesizer and the home-built electronics are based on homodyne detection after common-mode cancellation. Single-crystalline In_2Se_3 nanoribbons were grown inside a tube furnace using the Au nanoparticle-catalyzed vapor-liquid-solid growth method. The nanoribbons were mechanically transferred from the growth substrate onto 170nm SiN_x on doped Si substrates or 50nm SiN_x membrane TEM grids. In/Au (50 nm In and 100 nm Au) is used as the contact metal, which we found to form ohmic contact without any annealing. Characterization was done using SEM (FEI XL30 Sirion), TEM (Philips CM20-FEG), and AFM (Digital Instruments, Veeco Multimode SPM). The 2-terminal transport properties of the In_2Se_3 nanoribbon devices were measured by a probe station (Janis Research Inc., ST-4LF-2X-1Y-CX). Short voltage pulses were applied by a synthesized function generator (Stanford Research Systems, DS345).

S1. Comparison of various electrical probes

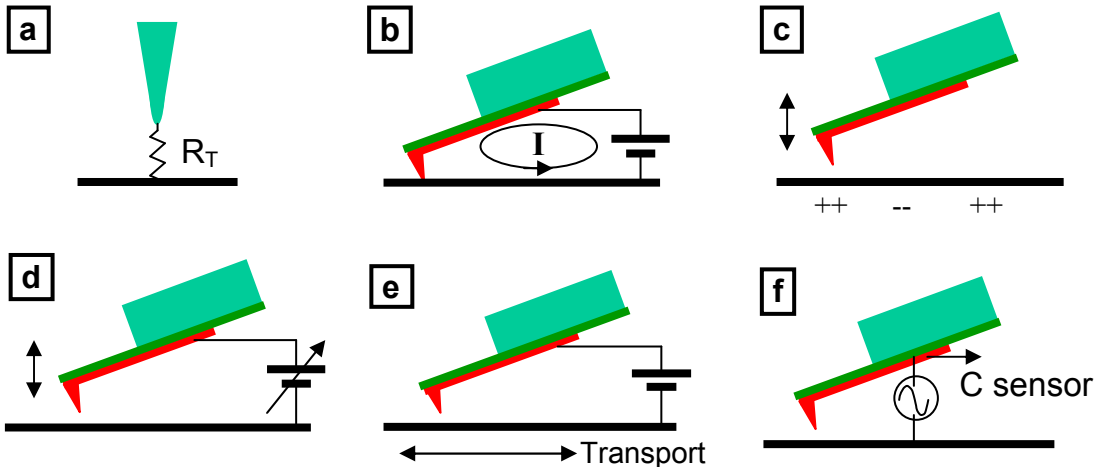

A number of well-established electrical scanning probe techniques are listed here for comparison with the scanning microwave impedance microscope (MIM) described in the main text. [a] Scanning tunneling microscope (STM) measures the tunneling current from the tip to a metallic sample. [b] Conductive atomic-force microscope (C-AFM) or scanning spreading resistance microscope (SSRM) maps out the DC current from the conductive tip to certain ohmic contacts on the sample. [c] Electrostatic force microscope (EFM) utilizes the cantilever and a force transducer to sense the electrostatic force. [d] Scanning Kelvin probe microscope (KPM) probes the surface potential distribution. [e] Scanning gate microscope uses the conductive tip as a local gate to perturb the transport property of the sample. [f] Scanning capacitance microscope measures the local tip-sample capacitance, usually under a sinusoidal gate bias that varies the depletion width.

Although all the above tools have been used in the literature to study local electrical properties, they are not suited to study the electronic inhomogeneity in In_2Se_3. First of all, the surface of In_2Se_3 is usually covered by an insulating layer, prohibiting the functioning of STM and C-AFM. Secondly, EFM and KPM require a substantial bias, which may already alter the sample state, to establish a potential distribution. Similarly, lateral transport is needed in SGM and the gate acts as a local perturbation. For all three probes, the results reveal the current path rather than the local conductivity, and conductive islands inside insulating matrix are difficult to probe. SCM is actually a prototype of microwave probe with poor shielding of the cantilever. Modulation of the tip-sample capacitance by varying depletion layer thickness is often needed to separate the signal from large background. Its use is therefore mainly limited in the semiconductor industry.

S2. Additional microwave images showing electronic inhomogeneity

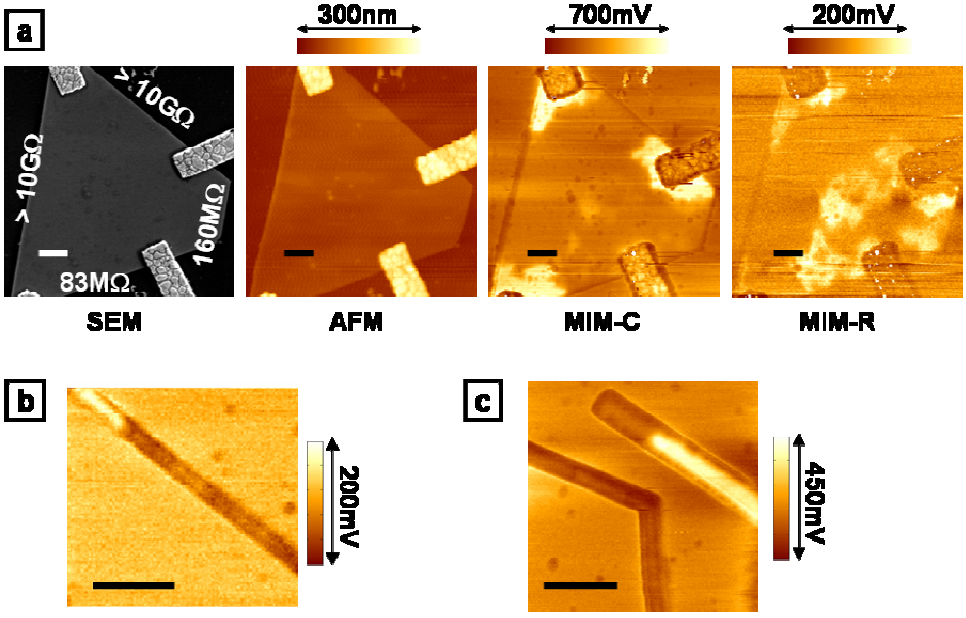

The inhomogeneous domain structures in In_2Se_3 nanoribbons are observed in many devices in this study. Figure S2 [a] shows the SEM, AFM, MIM-C, and MIM-R images of a large In_2Se_3 flake. The DC resistances between adjacent electrodes are labeled in the SEM image. Similar to the device shown in Figure 2, strong electronic inhomogeneity is seen in the MIM images. The relative contrast for the two microwave channels again follow the behavior discussed in the main text. In particular, the MIM data show that upper part of the flake is surrounded by highly resistive regions and electrically isolated from the rest of the sample. This is consistent with the fact that no appreciable DC conductance is measured from the upper electrode to the other three.

MIM-C images of several thin In_2Se_3 nano-ribbons are shown in Figure S2 [b]. Clear inhomogeneous domains are observed. The insulating regions appear darker than the background, an effect to be discussed in S6. All scale bars are 1μm.

S3. Effect of external voltage pulses

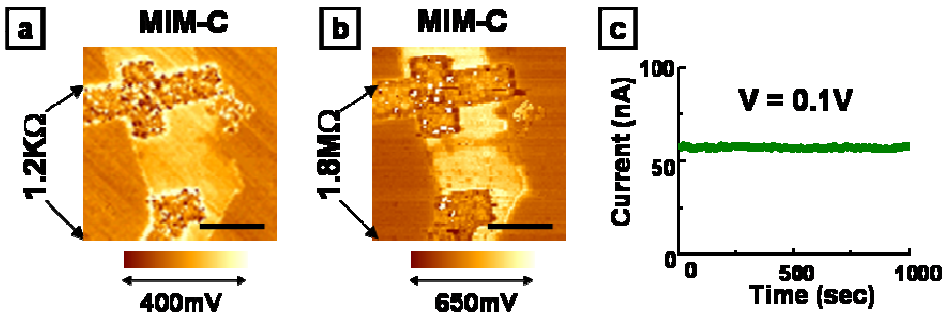

Voltage pulses were applied on the In_2Se_3 nanoribbon in figure 2 (main text). Resistances of the upper two sections increased from ~$10^5\Omega$ to ~$10^8\Omega$ (not shown) after the pretreatment. Resistance of the lowest section also increased from 1.2KΩ to 1.8MΩ, as shown here in S3 [a] and [b]. The MIM-C images taken after ([b]) the pulsing show a clear breakage of the high-conductivity path, which is not observed in [a] before the Joule heating. All scale bars are 2μm. Note that the two images were taken by different tips with different signal strength.

The DC resistance of the ribbon can also be monitored during the scanning. Figure S3 [c] shows the DC current through the two electrodes in [a] and [b] during the MIM scan. A constant bias of 0.1V is applied across the ribbon and its resistance is essentially unaltered by the MIM, suggesting a true noninvasive operation.

S4. I-AFM result

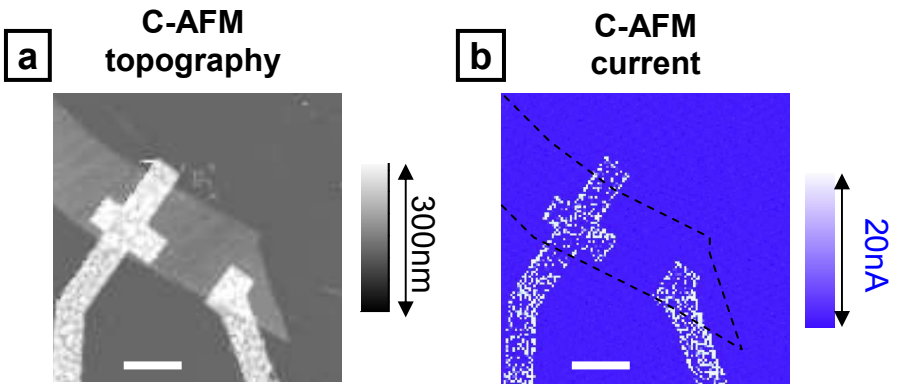

DC conductive AFM (C-AFM) result on the same ribbon in Figure 2 (main text) is shown here. The topography ([a]) and DC current ([b]) are simultaneously taken on the lower half of this ribbon. All scale bars are 2μm. The DC bias between the Pt/Ir coated Si tip and the In/Au leads is 0.2V and a 4MΩ current-limiting resistor is connected in the circuit. The dashed lines in [b] mark the location of the ribbon, which is invisible in the C-AFM current image due to the surface insulating layer. In fact, the current should be ~10nA on the ribbon and discernible in [b] if good Ohmic contact is formed between the Pt/Ir tip and the ribbon.

S5. Image process in the presence of metal electrodes

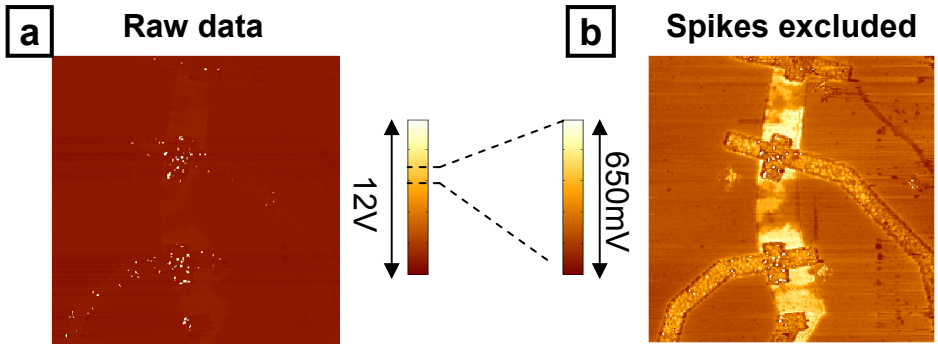

The macroscopic In/Au electrodes present very low impedance to ground. As the tip touches these bulk metals, the tip-sample interaction can not be viewed as a small perturbation to the original open circuit Z_{tip} any more. The microwave electronics usually generate huge output spikes due to short circuit to ground or instantaneous tunneling.

Figure S5 [a] shows the raw data after removing a slow varying background. The nanoribbon is barely visible due to the huge resistance spikes on the contacts. We limit the color scale to be part of the raw image and exclude spiky spots above and below it. The histogram corrected image is shown in [b]. Since the data on the electrodes are processed, we do not take them into account for any analysis.

S6. Simulation using finite-element analysis software

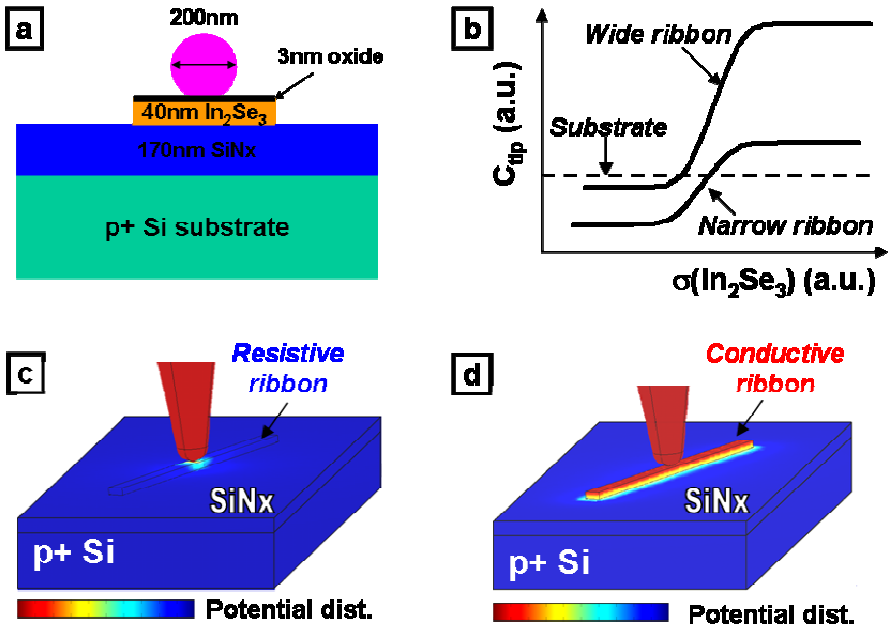

Simulation of the MIM signal is performed using a commercial finite-element analysis (FEA) program COMSOL 3.4 (COMSOL Inc., http://www.comsol.com/). Since the dimension of interest is much smaller than the radiation wavelength, the lumped-element model is accurate to describe the tip-sample interaction. We use quasi-static mode and time-harmonic (f = 1GHz) analysis to calculate the tip-ground admittance for a given geometry. The 2D axisymmetric mode is employed for wide ribbons with width >> the tip size, as shown in [a]. The following parameters are assumed in the simulation – tip radius r = 100nm; In_2Se_3 sample width w = 2μm and thickness t = 40nm; surface insulating layer d = 3nm; dielectric constant ε_r = 11 (bulk α-phase In_2Se_3); SiNx thickness 170nm and dielectric constant 7.5.

3D FEA simulation ([c] and [d]) has to be used to model the microwave response on narrow ribbons (w comparable to the tip diameter). Two typical simulation results of the tip-sample capacitance (C_{tip}) as a function of the sample conductivity σ are shown in Fig. S6[b]. In general, C_{tip} for both wide and narrow ribbons increases with increasing σ, while intersecting differently relative to that on the SiNx substrate. As a result, highly resistive narrow ribbons actually appear darker than the substrate (smaller C_{tip}) rather than displaying weak contrast over the background. This effect is clearly seen in Fig. 4[b] and Fig. S2[b] and [c].

S7. Metallic vs. insulating temperature dependence

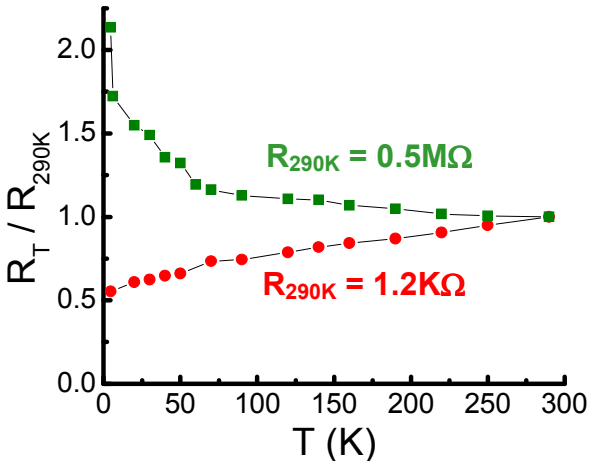

The temperature dependence of the resistance provides the information of the electronic state. For a typical highly conductive In_2Se_3 nanoribbon with R=1.2KΩ at the room temperature, the resistance decreases with decreasing temperatures (red dots), indicative of metallic behaviors. For the ribbon with room temperature R=0.5MΩ, on the other hand, a semiconducting behavior is observed in that the resistance increases with decreasing temperatures (green squares).